

## Supplementary Material

### Effect of reduced graphene oxide on the structural, optical, adsorption and photocatalytic property of iron oxide nanoparticles

R. Suresh<sup>a</sup>, R. Udayabhaskar<sup>b</sup>, Claudio Sandoval<sup>a</sup>, Eimmy Ramírez<sup>a</sup>, R.V. Mangalaraja<sup>b</sup>, Héctor D. Mansilla<sup>c</sup>, David Contreras<sup>ad</sup>, and Jorge Yañez<sup>a\*</sup>

<sup>a</sup>*Department of Analytical and Inorganic Chemistry, Faculty of Chemical Sciences, University of Concepción, Chile.*

<sup>b</sup>*Advanced Ceramics and Nanotechnology Laboratory, Department of Materials Engineering, Faculty of Engineering, University of Concepcion, Concepción, Chile.*

<sup>c</sup>*Department of Organic Chemistry, Faculty of Chemical Sciences, University of Concepción, Concepción, Chile.*

<sup>d</sup>*Centre for Biotechnology, University of Concepcion, Concepción, Chile*

\*Corresponding author. Tel: +56-41-2204329, E-mail: [jyanez@udec.cl](mailto:jyanez@udec.cl) (Jorge Yañez).

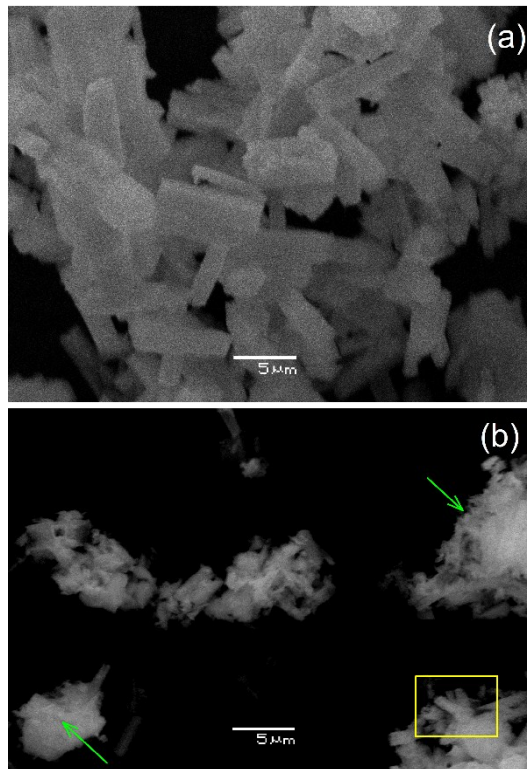


**Fig. S1:** SEM image of (a) pure  $\text{Fe}_2\text{O}_3$  and (b) 5%rGO@ $\text{Fe}_2\text{O}_3$  hybrid. Arrow mark indicates the deposition of rGO on  $\text{Fe}_2\text{O}_3$  particles. Rectangular mark point outs  $\text{Fe}_2\text{O}_3$  rods.

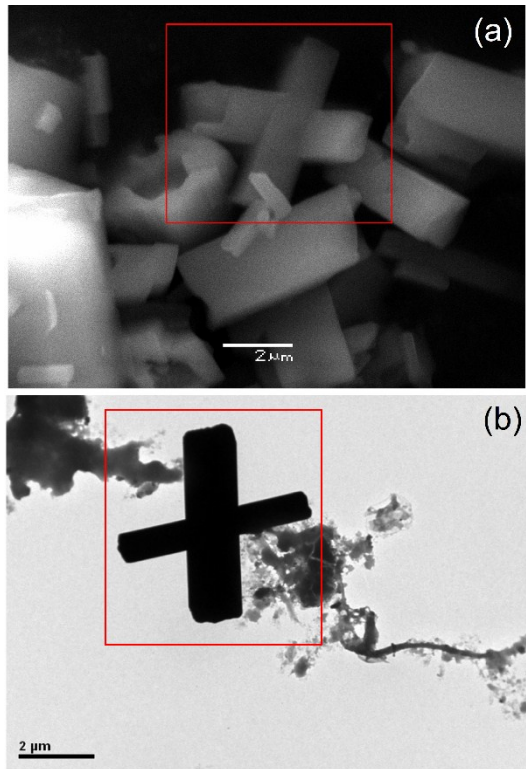


**Fig. S2:** (a) SEM and (b) TEM image of ferrous oxalate.

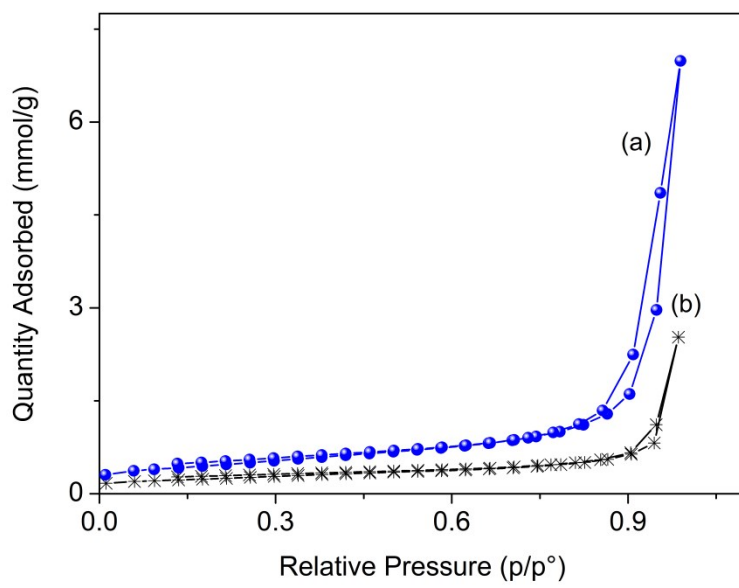


**Fig. S3:**  $\text{N}_2$  adsorption-desorption isotherms of (a) pure  $\text{Fe}_2\text{O}_3$  and (b) 5%rGO@ $\text{Fe}_2\text{O}_3$  hybrid.

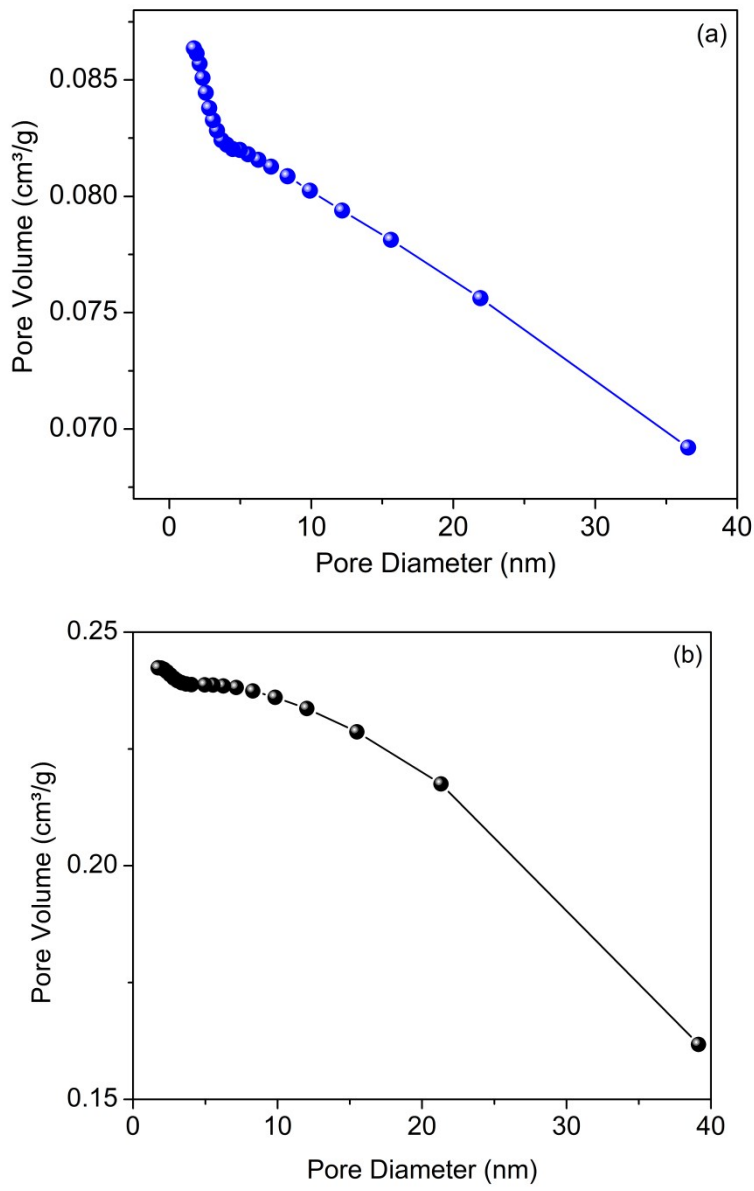


**Fig. S4:** Pore size distribution curve of (a) pure  $\text{Fe}_2\text{O}_3$  and (b) 5%rGO@ $\text{Fe}_2\text{O}_3$  hybrid.

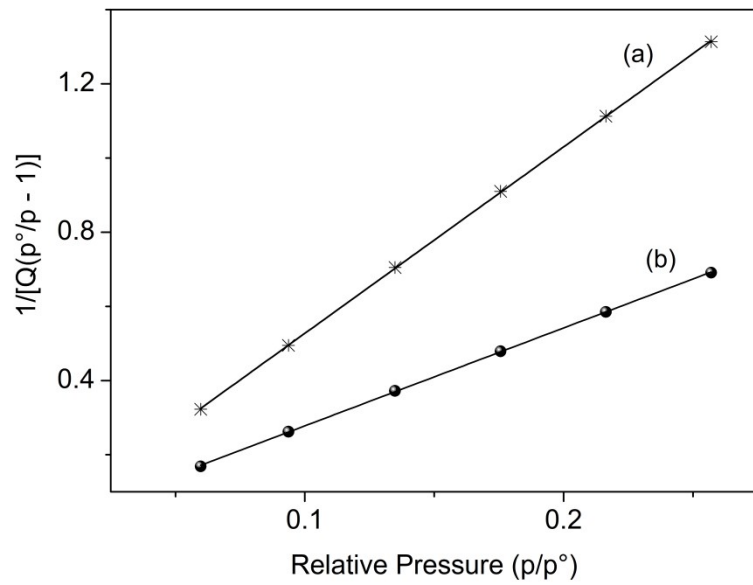


**Fig. S5:** BET surface area plot of (a) pure  $\text{Fe}_2\text{O}_3$  and (b) 5%rGO@ $\text{Fe}_2\text{O}_3$  hybrid.

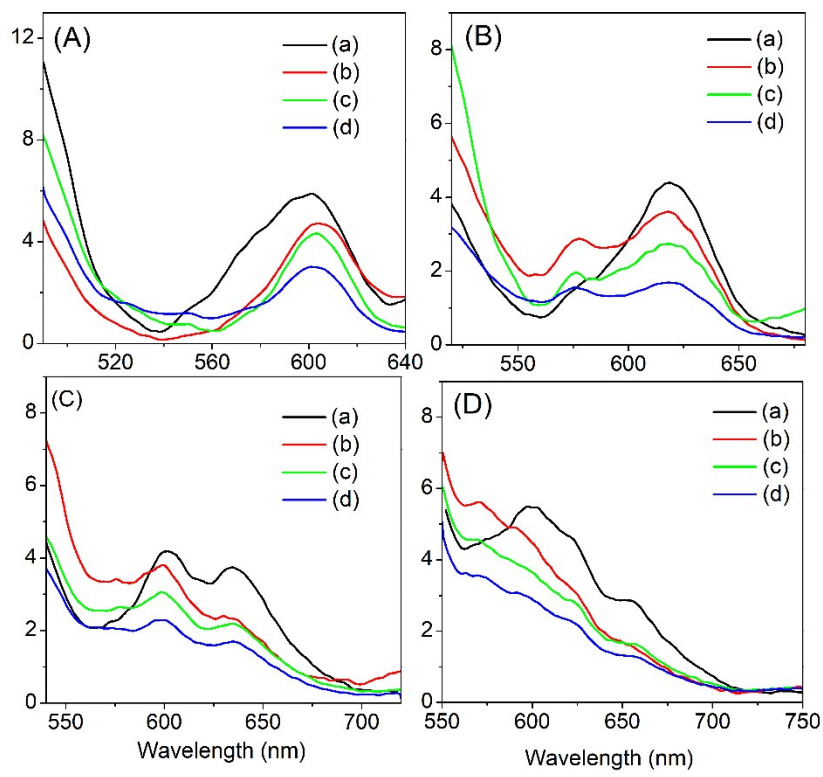


**Fig. S6:** PL spectrum of (a) pure  $\text{Fe}_2\text{O}_3$ , (b) 1%rGO@ $\text{Fe}_2\text{O}_3$ , (c) 3%rGO@ $\text{Fe}_2\text{O}_3$  and (d) 5%rGO@ $\text{Fe}_2\text{O}_3$  hybrid at (A) 460 nm, (B) 480 nm (C) 500 nm and (D) 520 nm excitations.

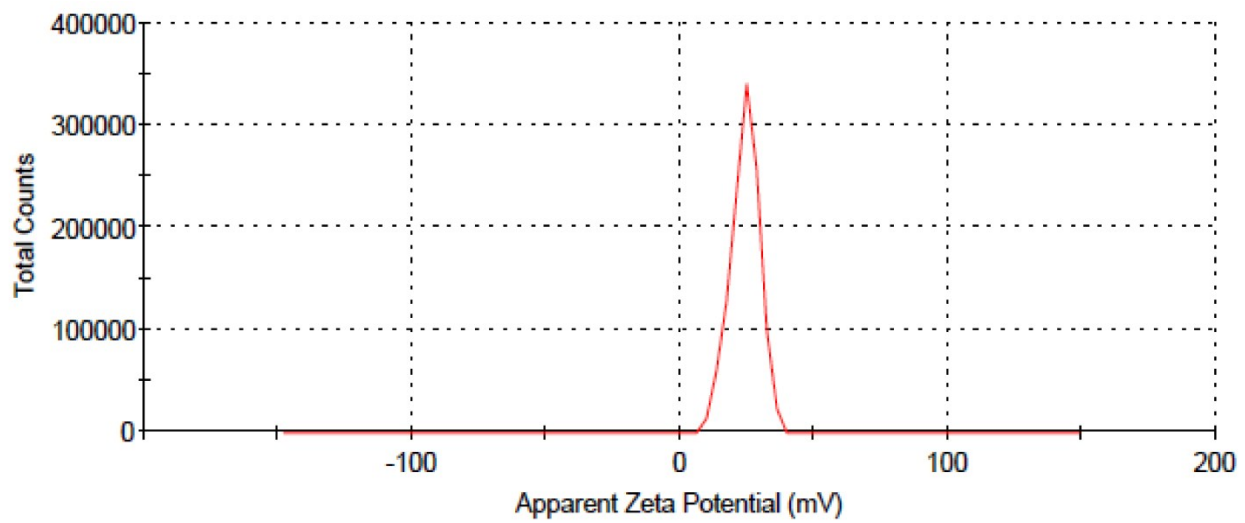


**Fig. S7:** Zeta potential distribution curve of 5%rGO@Fe<sub>2</sub>O<sub>3</sub> hybrid

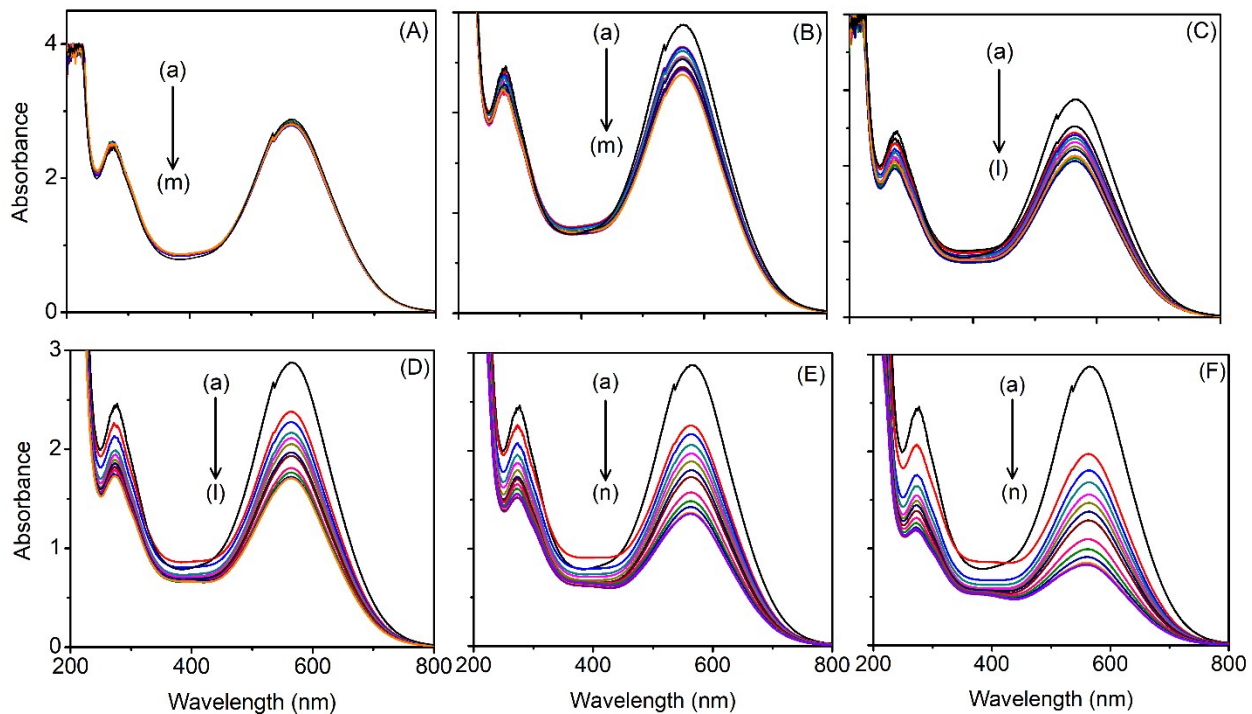


**Fig. S8:** UV visible spectrum of  $\text{AB}_{113}$  (100 ppm, 100 mL) after different contact time with (A) 20 mg, (B) 40 mg, (C) 60 mg (D) 80 mg (E) 100 mg and (F) 150 mg of 5%rGO@ $\text{Fe}_2\text{O}_3$  hybrid. (a) 10, (b) 20, (c) 30, (d) 40, (e) 50, (f) 65, (g) 80, (h) 140, (i) 200, (j) 260, (k) 320, (l) 380, (m) 440, and (n) 500 min.

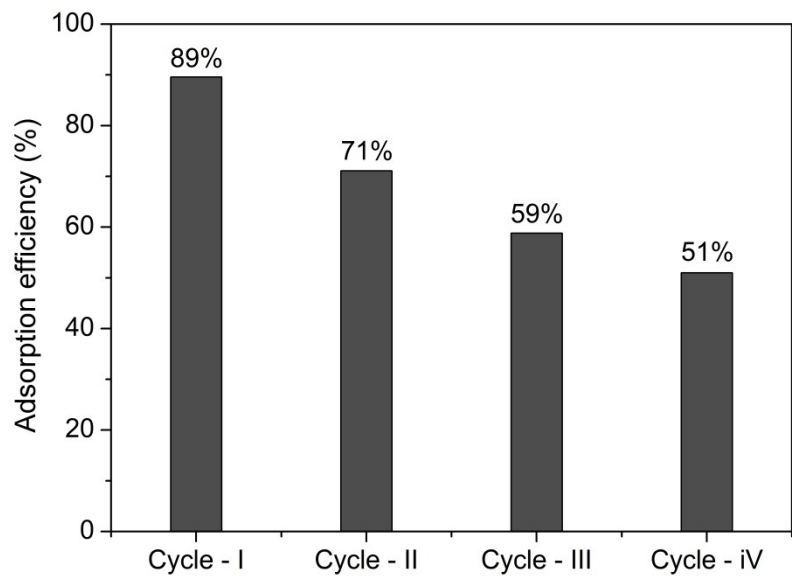


**Fig. S9:** Cyclic adsorption behavior of 5%rGO@Fe<sub>2</sub>O<sub>3</sub> hybrid

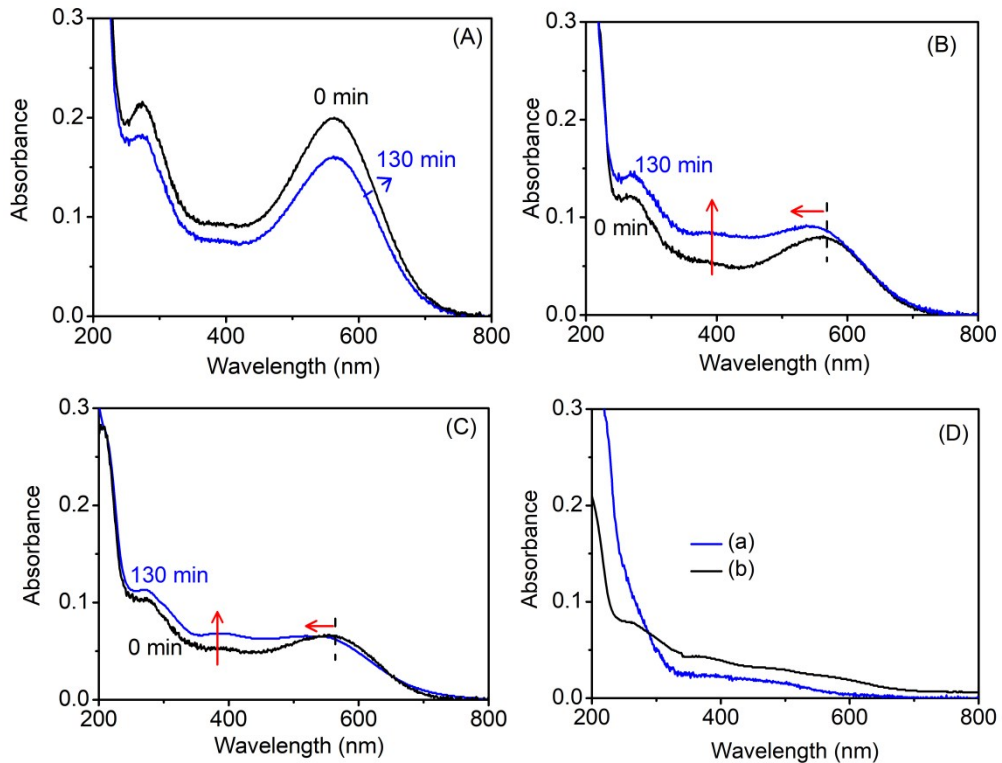


**Fig. S10:** UV visible spectra of AB<sub>113</sub> (7 mg L<sup>-1</sup>, 100 mL) in presence of (A) 5 mg, (B) 10 mg and (C) 15 of 5%rGO@Fe<sub>2</sub>O<sub>3</sub>hybrid. Figure D: UV visible spectra of AB<sub>113</sub> (7 mg L<sup>-1</sup>, 100 mL) in presence of 20 mg of 5%rGO@Fe<sub>2</sub>O<sub>3</sub>hybrid and visible light intensity with (a) 180 mW/cm<sup>2</sup> and (b) 2.2 mW/cm<sup>2</sup>.